

$\Xi_c - \Xi'_c$ mixing From Lattice QCD

Hang Liu,¹ Liuming Liu,^{2,3} Peng Sun,^{2,3} Wei Sun,⁴ Jin-Xin Tan,¹ Wei Wang,^{1,5,*} Yi-Bo Yang,^{6,7,8,3} and Qi-An Zhang^{9,†}

¹*INPAC, Key Laboratory for Particle Astrophysics and Cosmology (MOE),
Shanghai Key Laboratory for Particle Physics and Cosmology,*

²*School of Physics and Astronomy, Shanghai Jiao Tong University, Shanghai 200240, China*

²*Institute of Modern Physics, Chinese Academy of Sciences, Lanzhou, 730000, China*

³*University of Chinese Academy of Sciences, Beijing 100049, China*

⁴*Institute of High Energy Physics, Chinese Academy of Sciences, Beijing 100049, China*

⁵*Southern Center for Nuclear-Science Theory (SCNT), Institute of Modern Physics,
Chinese Academy of Sciences, Huizhou 516000, Guangdong Province, China*

⁶*CAS Key Laboratory of Theoretical Physics, Institute of Theoretical Physics,
Chinese Academy of Sciences, Beijing 100190, China*

⁷*School of Fundamental Physics and Mathematical Sciences,
Hangzhou Institute for Advanced Study, UCAS, Hangzhou 310024, China*

⁸*International Centre for Theoretical Physics Asia-Pacific, Beijing/Hangzhou, China*

⁹*School of Physics, Beihang University, Beijing 102206, China*

In heavy quark limit, the lowest-lying charmed baryons with two light quarks can form an SU(3) triplet and sextet. The Ξ_c in the SU(3) triplet and Ξ'_c in the sextet have the same J^{PC} quantum number and can mix due to the finite charm quark mass and the fact the strange quark is heavier than the up/down quark. We explore the Ξ_c - Ξ'_c mixing by calculating the two-point correlation functions of the Ξ_c and Ξ'_c baryons from lattice QCD. Based on the lattice data, we adopt two independent methods to determine the mixing angle between Ξ_c and Ξ'_c . After making the chiral and continuum extrapolation, it is found that the mixing angle θ is $1.2^\circ \pm 0.1^\circ$, which seems insufficient to account for the large SU(3) symmetry breaking effects found in weak decays of charmed baryons.

I. INTRODUCTION

Heavy baryons with a bottom or charm quark provide an ideal place to study the underlying theory for strong interactions. In heavy quark limit, charmed baryons can be elegantly classified according to heavy quark spin symmetry [1, 2]. Ground states of baryons with one heavy quark can be categorized into two sets: if the light quark system is spinless, three baryons form an SU(3) triplet; if the spin of the light quark system is one, then six charmed baryons form a sextet. However in reality, since the charm quark mass is finite and the strange quark is heavier than the up/down quark, charm baryons in the triplet and sextet are likely to mix with each other. An explicit realization is the $\Xi_c - \Xi'_c$ mixing, which is a direct consequence of the effective heavy quark and flavor SU(3) symmetry breaking.

Weak decays of charmed baryons also contribute to the understanding of the electroweak sector of the standard model. In particular semileptonic decays of charmed baryons are valuable to extract the CKM matrix element $|V_{cs}|$ (for some recent experimental measurements and lattice QCD calculations, please see Refs. [3–7] and many references therein). It is interesting to notice that based on the experimental measurements the flavor SU(3) symmetry, which is a very useful tool widely applied in the analysis of weak decays of heavy mesons, is found to be

sizably broken [8]. Various mechanisms to explain this observation were explored in Ref. [8] and a competitive explanation is through the $\Xi_c - \Xi'_c$ mixing [9]. Very interestingly, several recent works are devoted to determine the mixing angle from various methods, but the results are controversial. Based on experimental data on weak decays of Ξ_c and Ξ_{cc} , it is found that a large mixing angle is called for: $\theta = 24.66^\circ \pm 0.90^\circ$ in Ref.[9, 10] and $16.27^\circ \pm 2.30^\circ$ in Ref.[11]. A direct calculation in QCD sum rule gives $\theta = 5.5^\circ \pm 1.8^\circ$ [12], while in heavy-quark effective theory, it is found $\theta = 8.12^\circ \pm 0.80^\circ$ [13]. Besides, an earlier lattice QCD exploration indicates a small mixing angle [14].

This paper presents an update-to-date exploration of the $\Xi_c - \Xi'_c$ mixing from lattice QCD. Using the recently generated lattice configurations, we calculate the matrix elements $\langle 0 | O_{\Xi_c^{(3,6)}}(t) O_{\Xi_c^{(3,6)}}(0) | 0 \rangle$, where $O_{\Xi_c^3}$ and $O_{\Xi_c^6}$ denote the interpolators for the anti-triplet and sextet baryon respectively. With the results for the correlation function matrix, we use the direct fitting method to fit the energy levels and the mixing angle. As a comparison, the lattice spectroscopy method will also be used. After extracting the mixing angles with different lattice spacings and pion masses, we extrapolate the result to the chiral and continuum limit. We finally find that the mixing angle is at the order of 1° , which is likely to indicate the necessity to include other SU(3) symmetry-breaking effects in Ξ_c decays.

The rest of this paper is organized as follows. The theoretical framework for the $\Xi_c - \Xi'_c$ mixing is collected in Sec. II. We present our lattice simulations of the two-

* Corresponding author: wei.wang@sjtu.edu.cn

† Corresponding author: zhangqa@buaa.edu.cn

point correlation functions in Sec.III and a determination of the mixing angle from a direct fit in Sec. IV. Sec. V gives an analysis of the mixing angle through solving the generalized eigenvalue problem. The conclusion of this work is given in Sec. VI.

II. $\Xi_c - \Xi'_c$ MIXING IN HEAVY QUARK EFFECTIVE THEORY

In quark model, a baryon is made of three quarks. In heavy quark limit, heavy baryons with one charm quark can be well classified according to the angular momentum J of light quark system. If the spin wave function of the light quark system is antisymmetric, i.e. $J_{qq} = 0$, the Fermi statistics and antisymmetric feature in color space require that the flavor wave function is also antisymmetric in $SU(3)_F$. This corresponds the decomposition $(3 \times 3)_{\text{antisymmetric}} = \bar{3}$. If $J_{qq} = 1$, the $SU(3)_F$ flavor wave function should be symmetric and hence transforms as $(3 \times 3)_{\text{symmetric}} = 6$.

In heavy quark effective theory (HQET) [1, 2], the generic interpolating operator of a heavy baryon takes the form $O = \epsilon^{abc} (q_1^{Ta} C \Gamma q_2^b) \Gamma' \tilde{Q}^c$, where $q_{1,2}$ denotes a light quark, and \tilde{Q} is the heavy quark field in HQET satisfying $\gamma^0 \tilde{Q} = \tilde{Q}$. In this interpolator we have explicitly specified the color indices a, b, c . The transposition T acts on a Dirac spinor, and $C = \gamma^0 \gamma^2$ is the charge conjugation matrix. Summing over the color indices with the totally antisymmetric tensor ϵ^{abc} results in a gauge invariant operator. The Dirac matrix Γ and Γ' are related to the internal spin structures of the heavy baryon. For the ground state, the angular momentum of light quark system is either 0 or 1. If $J = 0$ corresponds to the current $q_1^T C \gamma_5 q_2$, and $J = 1$ corresponds to $q_1^T C \vec{\gamma} q_2$. Therefore, the baryonic current $O_1 = (q_1^T C \gamma_5 q_2) \tilde{Q}$ corresponds to the spin 1/2 baryon, and the current $\vec{O}_2 = (q_1^T C \vec{\gamma} q_2) \tilde{Q}$ contains both spin-1/2 and spin-3/2 components. Using \vec{O}_2 , one can construct the spin-3/2 component $\vec{O}_2^{3/2} = \vec{O}_2 + \frac{1}{3} \vec{\gamma} \vec{\gamma} \cdot \vec{O}_2$ which satisfying the condition $\vec{\gamma} \cdot \vec{O}_2^{3/2} = 0$, and the spin-1/2 component $O_2^{1/2} = -\frac{1}{3} \vec{\gamma} \vec{\gamma} \cdot \vec{O}_2 = (q_1^T C \vec{\gamma} q_2) \cdot \vec{\gamma} \gamma_5 \tilde{Q}$.

As a result, one can obtain the baryonic currents of $SU(3)_F$ eigenstate as [25]

$$O^3 = \epsilon^{abc} (\ell^{Ta} C \gamma_5 s^b) P_+ \tilde{c}^c, \quad (1)$$

$$O^6 = \epsilon^{abc} (\ell^{Ta} C \vec{\gamma} s^b) \cdot \vec{\gamma} \gamma_5 P_+ \tilde{c}^c, \quad (2)$$

with $\ell = (u, d)$. $P^+ = (1 + \gamma^0)/2$ is the positive parity

projector.

If the finite charm quark mass and the differences between the strange quark and up/down quark are taken into account, the two Ξ_c states can mix and their mixing effect could be described by a 2×2 mixing matrix:

$$\begin{pmatrix} |\Xi_c\rangle \\ |\Xi'_c\rangle \end{pmatrix} = \begin{pmatrix} \cos \theta & \sin \theta \\ -\sin \theta & \cos \theta \end{pmatrix} \begin{pmatrix} |\Xi_c^3\rangle \\ |\Xi_c^6\rangle \end{pmatrix}, \quad (3)$$

where θ denotes the mixing angle. The mass eigenstates are orthogonal:

$$H_{\text{QCD}} |\Xi_c\rangle = m_{\Xi_c} |\Xi_c\rangle, \quad H_{\text{QCD}} |\Xi'_c\rangle = m_{\Xi'_c} |\Xi'_c\rangle, \quad (4)$$

where $m_{\Xi_c}/m_{\Xi'_c}$ denote the physical baryon masses.

III. TWO-POINT CORRELATION FUNCTION FROM LATTICE QCD

The simulations in this work will be performed on the gauge configurations generated by the Chinese Lattice QCD (CLQCD) collaboration with $N_f = 2 + 1$ flavor stout smeared clover fermions and Symanzik gauge action, at three lattice spacings and three pion masses including the physical one. The detailed parameters are listed in Table I. Some previous applications of these configurations can be found in Refs. [7, 26–28].

In the numerical simulation, to improve the signal-to-noise ratio of the simulation, we generate the f -flavored wall source to point sink propagators

$$S_{w-p}^f(\vec{x}, t, t_0; \vec{p}) = \sum_{\vec{x}_s} e^{-i\vec{p} \cdot (\vec{x} - \vec{x}_s)} S^f(\vec{x}, t; \vec{x}_s, t_0) \quad (5)$$

on the Coulomb gauge fixed configurations. S^f denotes the propagator from wall source at $(\sum_{\vec{x}_s} \vec{x}_s, t_0)$ to the point sink (\vec{x}, t) . We consider the 2×2 correlation function matrix

$$\mathcal{C}(t, t_0) = \sum_{\vec{x}} \begin{pmatrix} \langle O_p^3(\vec{x}, t) \bar{O}_w^3(\vec{0}, t_0) \rangle & \langle O_p^3(\vec{x}, t) \bar{O}_w^6(\vec{0}, t_0) \rangle \\ \langle O_p^6(\vec{x}, t) \bar{O}_w^3(\vec{0}, t_0) \rangle & \langle O_p^6(\vec{x}, t) \bar{O}_w^6(\vec{0}, t_0) \rangle \end{pmatrix} \quad (6)$$

that contains the baryonic currents. The subscript “ w ” and “ p ” denote the wall source and point sink. The related two-point functions can be constructed by the light, strange, and charm quark propagators $S_{w-p}^{\{l,s,c\}}$ with momentum $\vec{p} = \vec{0}$

$$C_{11}(t, t_0) = - \sum_{\vec{x}} \epsilon^{abc} \epsilon^{a'b'c'} \left(S_{w-p}^l(\vec{x}, t, t_0) \right)_{\alpha\alpha'}^{aa'} \left(C \gamma_5 S_{w-p}^s(\vec{x}, t, t_0) \gamma_5 C \right)_{\alpha\alpha'}^{bb'} \left(P_+ S_{w-p}^c(\vec{x}, t, t_0) P_+ T \right)_{\alpha\alpha'}^{cc'}, \quad (7)$$

Ensemble	β	$L^3 \times T$	a (fm)	m_l^b	m_s^b	m_c^b	m_π	N_{meas}
C11P14L		$48^3 \times 96$		-0.2825	-0.2310	0.4800	135	203×48
C11P22M	6.20	$32^3 \times 64$	0.108	-0.2790	-0.2310	0.4800	222	451×20
C11P29S		$24^3 \times 72$		-0.2770	-0.2315	0.4780	284	432×26
C08P30S	6.41	$32^3 \times 96$	0.080	-0.2295	-0.2010	0.2326	297	653×26
C06P30S	6.72	$48^3 \times 144$	0.055	-0.1850	-0.1687	0.0770	312	136×80

TABLE I. Parameters of the ensembles used in this work, including the gauge coupling $\beta = 10/g^2$, the 4-dimensional volume $L^3 \times T$, lattice spacing a , bare quark masses $m_{l,s,c}^b$, pion mass m_π and total measurements N_{meas} . The total measurements are equal to the number of gauge configurations times the measurements from different time slices on one configuration.

$$C_{12}(t, t_0) = \sum_{\vec{x}} \epsilon^{abc} \epsilon^{a'b'c'} \sum_{i=1,2,3} \left(S_{w-p}^l(\vec{x}, t, t_0) \right)_{\alpha\alpha'}^{aa'} \left(C \gamma_5 S_{w-p}^s(\vec{x}, t, t_0) \gamma^i C \right)_{\alpha\alpha'}^{bb'} \left(P_+ S_{w-p}^c(\vec{x}, t, t_0) \gamma^i \gamma_5 P_+ T \right)^{cc'}, \quad (8)$$

$$C_{21}(t, t_0) = - \sum_{\vec{x}} \epsilon^{abc} \epsilon^{a'b'c'} \sum_{i=1,2,3} \left(S_{w-p}^l(\vec{x}, t, t_0) \right)_{\alpha\alpha'}^{aa'} \left(C \gamma^i S_{w-p}^s(\vec{x}, t, t_0) \gamma_5 C \right)_{\alpha\alpha'}^{bb'} \left(P_+ \gamma^i \gamma_5 S_{w-p}^c(\vec{x}, t, t_0) P_+ T \right)^{cc'}, \quad (9)$$

$$C_{22}(t, t_0) = \sum_{\vec{x}} \epsilon^{abc} \epsilon^{a'b'c'} \sum_{i,j=1,2,3} \left(S_{w-p}^l(\vec{x}, t, t_0) \right)_{\alpha\alpha'}^{aa'} \left(C \gamma^i S_{w-p}^s(\vec{x}, t, t_0) \gamma^j C \right)_{\alpha\alpha'}^{bb'} \left(P_+ \gamma^i \gamma_5 S_{w-p}^c(\vec{x}, t, t_0) \gamma^j \gamma_5 P_+ T \right)^{cc'} \quad (10)$$

where the subscript α, α' denote the Dirac indices and superscript a, b, c, a', b', c' denote the color indices. In the above a trace has been taken and we have adopted a unpolarized projector $T = (1 + \gamma^0)/2$. One can generate the wall source propagators at several time slices t_0 and then average the two-point functions constructed by these propagators, so that the statistical precisions of numerical results on different ensembles can reach the same level. The explicit statistics on each ensemble, including the number of gauge configurations and the mea-

surements from different time slices on one configuration, are collected in Table I.

One can extract the mixing parameters from a joint analysis of both diagonal and non-diagonal terms of \mathcal{C} . In the correlation functions, one can insert the mass eigenstates $|n\rangle$ and convert them to local matrix elements. The mismatch of flavor basis baryonic currents and mass eigenstates will be related to the mixing angle under the mixing pattern in Eq.(3). For example, the correlation C_{11} is given as:

$$\begin{aligned} C_{11}(t, t_0) &= \sum_{\vec{x}} \langle O_p^{\bar{3}}(\vec{x}, t) \bar{O}_w^{\bar{3}}(\vec{0}, t_0) \rangle \\ &= \sum_{n=\Xi_c, \Xi'_c, \dots} \frac{e^{-m_n(t-t_0)}}{(La)^3 (2m_n)} \langle 0 | O_p^{\bar{3}}(\vec{0}, 0) | n \rangle \langle n | \bar{O}_w^{\bar{3}}(\vec{0}, 0) | 0 \rangle \\ &= \frac{1}{(La)^3} \left[\frac{e^{-m_{\Xi_c}(t-t_0)}}{2m_{\Xi_c}} \langle 0 | O_p^{\bar{3}}(\vec{0}, 0) | \Xi_c \rangle \langle \Xi_c | \bar{O}_w^{\bar{3}}(\vec{0}, 0) | 0 \rangle + \frac{e^{-m_{\Xi'_c}(t-t_0)}}{2m_{\Xi'_c}} \langle 0 | O_p^{\bar{3}}(\vec{0}, 0) | \Xi'_c \rangle \langle \Xi'_c | \bar{O}_w^{\bar{3}}(\vec{0}, 0) | 0 \rangle + \dots \right]. \end{aligned} \quad (11)$$

From this expression one can in general determine the mass of the ground state with a large time slice t . The

excited state contributions are greatly suppressed in this regime, and the correlation functions become

$$C_{11}(t, t_0) = \frac{1}{(La)^3} \left[\frac{e^{-m_{\Xi_c}(t-t_0)}}{2m_{\Xi_c}} \langle 0 | O_p^{\bar{3}}(\vec{0}, 0) | \Xi_c \rangle \langle \Xi_c | \bar{O}_w^{\bar{3}}(\vec{0}, 0) | 0 \rangle + \frac{e^{-m_{\Xi'_c}(t-t_0)}}{2m_{\Xi'_c}} \langle 0 | O_p^{\bar{3}}(\vec{0}, 0) | \Xi'_c \rangle \langle \Xi'_c | \bar{O}_w^{\bar{3}}(\vec{0}, 0) | 0 \rangle \right]$$

$$\begin{aligned}
&= \frac{1}{(La)^3} \left[\frac{e^{-m_{\Xi_c}(t-t_0)}}{2m_{\Xi_c}} \left\langle 0 \left| O_p^3(\vec{0}, 0) \left(\left| \Xi_c^3 \right\rangle \cos \theta + \left| \Xi_c^6 \right\rangle \sin \theta \right) \left(\left\langle \Xi_c^3 \right| \cos \theta + \left\langle \Xi_c^6 \right| \sin \theta \right) \left| \bar{O}_w^3(\vec{0}, 0) \right| 0 \right\rangle \right. \right. \\
&\quad \left. \left. + \frac{e^{-m_{\Xi'_c}(t-t_0)}}{2m_{\Xi'_c}} \left\langle 0 \left| O_p^3(\vec{0}, 0) \left(- \left| \Xi_c^3 \right\rangle \sin \theta + \left| \Xi_c^6 \right\rangle \cos \theta \right) \left(- \left\langle \Xi_c^3 \right| \sin \theta + \left\langle \Xi_c^6 \right| \cos \theta \right) \left| \bar{O}_w^3(\vec{0}, 0) \right| 0 \right\rangle \right] \right] \\
&\equiv A_p A_w^\dagger \left[\frac{\cos^2 \theta}{2m_{\Xi_c}} e^{-m_{\Xi_c}(t-t_0)} + \frac{\sin^2 \theta}{2m_{\Xi'_c}} e^{-m_{\Xi'_c}(t-t_0)} \right], \tag{12}
\end{aligned}$$

where the t -independent parameter $A_{p/w} = (La)^{-3/2} \langle 0 | O_{p/w}^3(\vec{0}, 0) | \Xi_c^3 \rangle$. In the second step, we have used the mixing matrix in Eq. (3). Similarly, the other matrix elements can be expressed as

$$C_{12}(t, t_0) = \sum_{\vec{x}} \langle O_p^3(\vec{x}, t) \bar{O}_w^6(\vec{0}, t_0) \rangle = A_p B_w^\dagger \left[\frac{\cos \theta \sin \theta}{2m_{\Xi_c}} e^{-m_{\Xi_c}(t-t_0)} - \frac{\cos \theta \sin \theta}{2m_{\Xi'_c}} e^{-m_{\Xi'_c}(t-t_0)} \right], \tag{13}$$

$$C_{21}(t, t_0) = \sum_{\vec{x}} \langle O_p^6(\vec{x}, t) \bar{O}_w^3(\vec{0}, t_0) \rangle = B_p A_w^\dagger \left[\frac{\cos \theta \sin \theta}{2m_{\Xi_c}} e^{-m_{\Xi_c}(t-t_0)} - \frac{\cos \theta \sin \theta}{2m_{\Xi'_c}} e^{-m_{\Xi'_c}(t-t_0)} \right], \tag{14}$$

$$C_{22}(t, t_0) = \sum_{\vec{x}} \langle O_p^6(\vec{x}, t) \bar{O}_w^6(\vec{0}, t_0) \rangle = B_p B_w^\dagger \left[\frac{\sin^2 \theta}{2m_{\Xi_c}} e^{-m_{\Xi_c}(t-t_0)} + \frac{\cos^2 \theta}{2m_{\Xi'_c}} e^{-m_{\Xi'_c}(t-t_0)} \right], \tag{15}$$

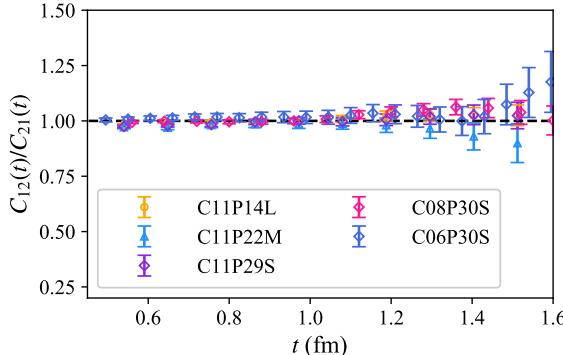


FIG. 1. Ratios of C_{12} and C_{21} as function of t on different ensembles. Their values are consistent with 1 indicate the lattice artifacts generated by wall source are independent of the mixing in the flavor space.

with $B_{p/w} = (La)^{-3/2} \langle 0 | O_{p/w}^6(\vec{0}, 0) | \Xi_c^6 \rangle$. It should be noticed that the lattice artifacts generated by the wall source and point sink have been collected into the local matrix elements $A_{p/w}$ and $B_{p/w}$, and would not contaminate the energy eigenstates and their mixing. Illustrated as Fig.1, the ratios C_{12}/C_{21} are consistent with 1 for all the ensembles we used in this calculation, regardless of the pion masses and lattice spacings. Such an observation indicates that the color-spacial factor introduced by the wall source will contribute to an overall factor, which is independent of the mixing in the flavor space.

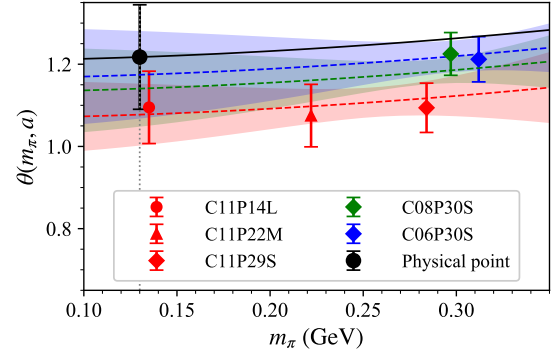


FIG. 2. Chiral and continuum extrapolations of θ based on the fit results of Eq.(16) as a function of m_π . The extrapolated results from chiral fits at fixed lattice spacings are shown as the red, green, and blue dashed lines with error bands. The black line corresponds to the chiral and continuum extrapolation. The black point denotes the extrapolated values at the physical pion mass and continuum limit. Uncertainties in all data points are statistical only.

IV. MIXING ANGLE FROM JOINT FIT

To extract the masses and mixing angle from the correlation functions, one can apply a joint fit based on the parametrization formula of the correlation function matrix in Eq.(12-15) with parameters A , B , m_{Ξ_c} , $m_{\Xi'_c}$ and θ at $t_0 = 0$.

	m_{Ξ_c} (GeV)	$m_{\Xi'_c}$ (GeV)	θ (°)	$\chi^2/\text{d.o.f}$	fit range (fm)
C11P14L	2.4256(19)	2.5196(22)	1.083(30)	0.96	1.19 – 2.81
C11P22M	2.4380(27)	2.5351(30)	0.988(49)	1.0	1.19 – 2.92
C11P29S	2.4587(27)	2.5536(29)	1.002(50)	1.1	1.19 – 3.24
C08P30S	2.4753(21)	2.5809(26)	1.080(42)	0.95	1.20 – 2.40
C06P30S	2.4695(37)	2.5815(48)	1.021(67)	1.2	1.32 – 2.40
Extrapolated	2.4380(68) _{stat} (403) _{syst}	2.5562(74) _{stat} (422) _{syst}	1.20(9) _{stat} (2) _{syst}		
Exp. data [29]	$2.46794^{+0.00017}_{-0.00020}$	2.5784 ± 0.0005	—		

TABLE II. Results of masses and mixing angles from correlated matrix fits on different ensembles, together with $\chi^2/\text{d.o.f}$ and fit ranges $t_{\min} - t_{\max}$ for each fits. The following are extrapolated results, where the experimental data are also listed for comparison.

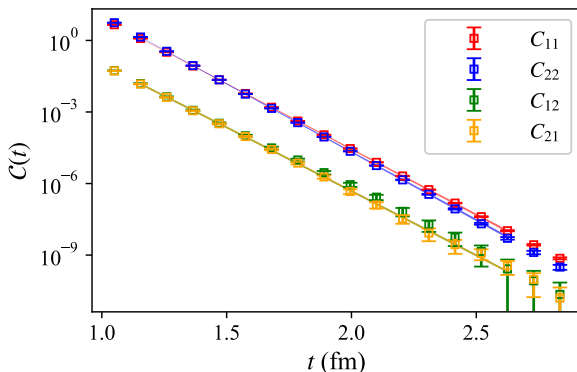


FIG. 3. Joint fit of the 2×2 correlation function matrix using Eq.(12-15). The data shown here are from C11P14L, the colored bands indicate the time range and fit results of each matrix element.

The choice of fit t -range relies on both fit quality and physical consideration: the starting time slices t_{\min} after which the data points are included in the fit must be chosen such that contributions from higher excited states have been suppressed sufficiently with the smallest possible statistical uncertainties. The t_{\max} are determined by avoiding the contaminations from backward-propagating in the periodic boundary condition and avoiding too many degrees of freedom in the χ^2 fit leading to poorly estimating. The optimal choices of the fit range are different for the different ensembles, so we determine them independently to obtain a reasonable description of the joint matrix fit.

Table II includes the fitted values of m_{Ξ_c} , $m_{\Xi'_c}$, θ and their statistical uncertainties, together with the correlated, reduced χ^2 -values ($\chi^2/\text{d.o.f}$) and fit ranges $t_{\min} - t_{\max}$ on each ensemble. Of all fits, we evaluate the fit qualities by $\chi^2/\text{d.o.f} \lesssim 1$ and the smallest uncertainties for the parameters. As an example, Fig.3 shows the correlated joint fit results on C11P14L, which is perfectly consistent with the data of correlation functions.

After extracting the mixing angles from the ensembles at different pion masses and lattice spacings, we can ex-

trapolate these results to the physical values of the quark masses and the continuum limit. We perform the chiral and continuum extrapolation through the following ansatz:

$$\theta(m_\pi, a) = \theta_{\text{phy}} + c_1 (m_\pi^2 - m_{\pi,\text{phy}}^2) + c_2 a^2, \\ m_n(m_\pi, a) = m_{n,\text{phy}} + c_1 (m_\pi^2 - m_{\pi,\text{phy}}^2) + c_2 a^2. \quad (16)$$

These extrapolations are performed at the next-to-leading-order in the chiral expansion. We also included a quadratic dependence of lattice spacings. In order to estimate the systematic uncertainties associated with this truncation, we add the higher-order analytic terms to the fit functions, such as the quartic term m_π^4 in chiral expansion, or a^3 term in continuum extrapolation. The latter one, which may arise from heavy-quark discretization errors, gives sizable systematic error. In practice, we introduce these terms into the fit functions Eq.(16) separately and calculate the extrapolated masses and mixing angle from the new higher-order fits. The extrapolated results with both statistic and systematic uncertainties from the higher-order analytic terms are collected in Table II.

With the extrapolation uncertainties taken into account, we find the masses for the Ξ_c and Ξ'_c are both consistent with the experimental data, while the mixing angle is:

$$\theta = (1.200 \pm 0.090 \pm 0.020)^\circ. \quad (17)$$

V. MIXING ANGLE FROM GENERALIZED EIGENVALUE PROBLEM

Besides the correlated fit, the mixing angle can be also extracted by solving the generalized eigenvalue problem (GEVP) [30, 31]

$$\mathcal{C}(t)v_n(t) = \lambda_n(t)\mathcal{C}(t_r)v_n(t), \quad (18)$$

where n labels the states of Ξ_c, Ξ'_c , $\lambda_n(t)$ is the eigenvalue and follows the boundary condition $\lambda_n(t_r) = 1$, and there

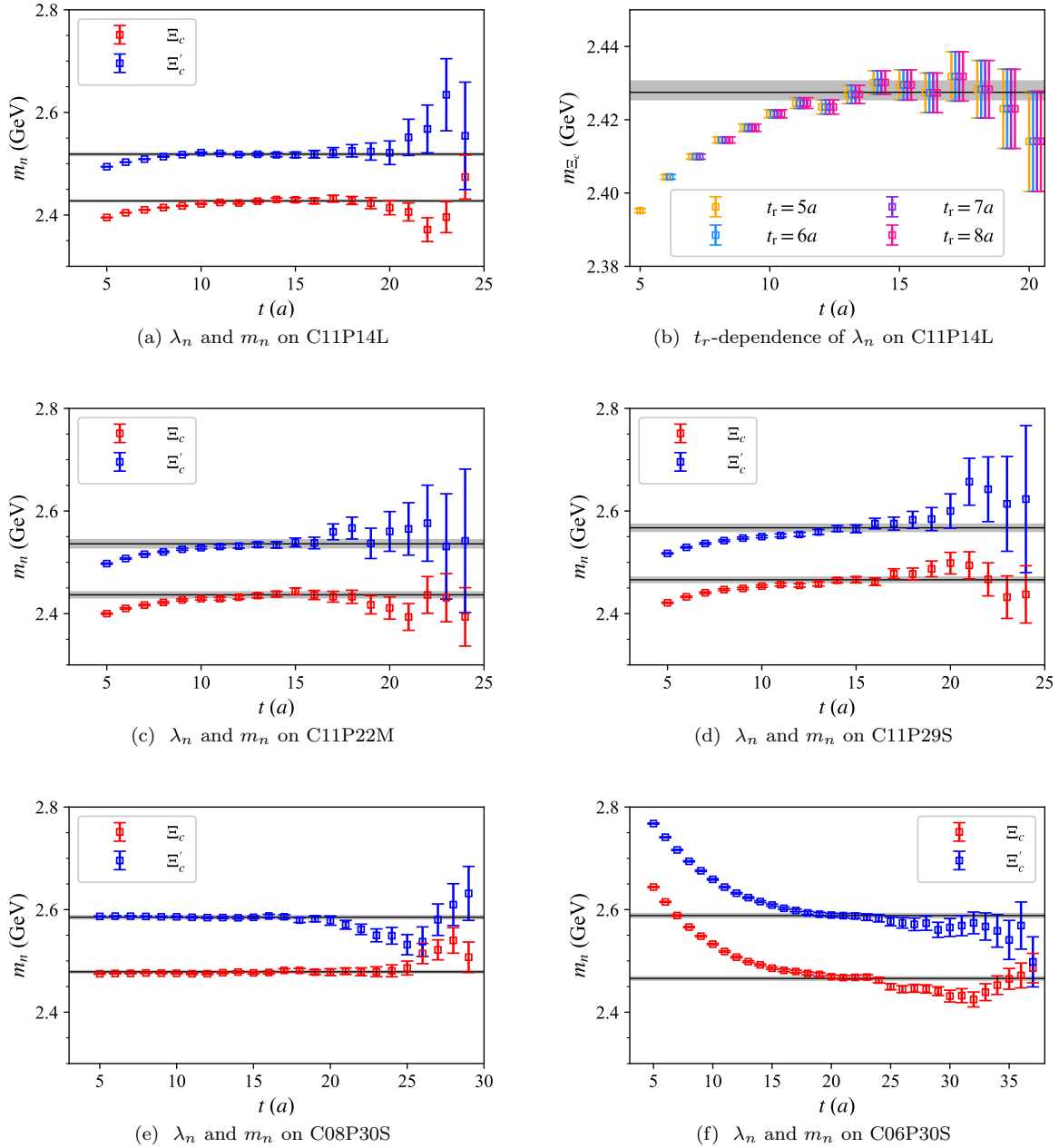


FIG. 4. (a, c-f) Effective masses from eigenvalues $\lambda_n(t)$ ($n = \Xi_c, \Xi'_c$), and their fit results on different ensembles. The eigenvalues are from solving the GEVP Eq.18 for the correlation function matrix at $t_r = 5a$. (b) t_r -dependence of λ_n on C11P14L, with $t_r = \{5, 6, 7, 8\}a$.

is an orthogonality condition for the eigenvectors of different states (n, n') as $v_n^\dagger \mathcal{C}(t_r) v_n = \delta_{nn'}$. This orthogonality condition allows us to extract the spectrum of near degenerate states Ξ_c and Ξ'_c . The eigenvalues λ_n and eigenvectors v_n usually be solved independently on each time slice t from the source at t_0 , while for the nearby masses, their eigenvalues might fluctuate time slice by time slice. So we choose a reference time slice t_r on which reference eigenvector as $v_{n,\text{ref}}$, and compare eigenvectors on other time slices by finding the maximum value of

$v_{n',\text{ref}}^\dagger \mathcal{C}(t_r) v_n$ which associates a state n with a reference state n' .

As discussed above, the two-point correlation function can be decomposed into a time-independent factor and $e^{-m_n t}$ at large times. In the first factor, the matrix element $\langle 0 | O^i | n \rangle$ is related to the eigenvectors which contain the mixing effects between the flavor and energy eigenstates, and the effective masses related to energy eigenstates can be extracted from the exponential behavior of the correlators λ_n . The fit function of masses can be

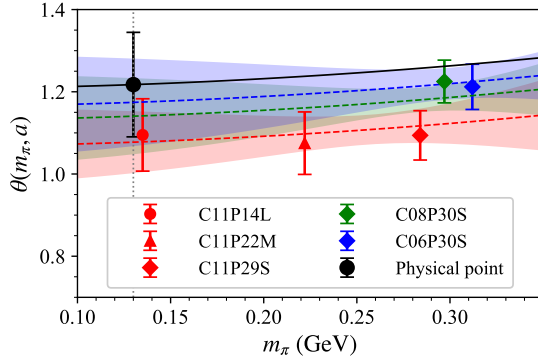


FIG. 5. Chiral and continuum extrapolations of θ extracted from GEVP method. The extrapolated results from chiral fits at fixed lattice spacings are shown as the red, green, and blue dashed lines with error bands. The black line corresponds to the chiral and continuum extrapolation. The black point denotes the extrapolated values at the physical pion mass and continuum limit. Errors in all data points are statistical only.

expressed as

$$\lambda_n(t) = c_0 e^{-m_n(t-t_r)} \left(1 + c_1 e^{-\Delta E(t-t_r)} \right), \quad (19)$$

where the fit parameters c_0 collect the contributions from time-independent factors and m_n denotes the effective mass of $n = (\Xi_c, \Xi'_c)$, c_1 and ΔE describe the higher excited states contributions which can be neglected at large time. By separating the nearby states, we perform two independent fits to extract the effective masses m_{Ξ_c} and $m_{\Xi'_c}$.

The extractions of effective masses on different ensembles are illustrated in Fig.4(a, c-f). In these plots, the effective masses $m_n = \log(\lambda_n(t)/\lambda_n(t+1))$ are calculated from the eigenvalues of GEVP at reference time slice $t_r = 5a$, and the error bands are determined from one-state fits (choosing $c_1 = 0$ and perform the fits at large t range) based on Eq.(19).

The fit results are collected in the upper left panel of Table III. In order to analyze the t_r dependence, we choose several reference time slices to extract and fit the effective masses. Shown as Fig.4(b), the selection of t_r hardly affects the results of effective masses.

After diagonalizing the correlation function matrix \mathcal{C} , we find the GEVP eigenvalues λ_n are degenerate to the energy basis, thereby the mixing effects will be collected into the GEVP eigenvectors v_n . From the parametrization form in Eq.(12-15), the normalized eigenvectors can be expressed as

$$v_1 = \sqrt{1 + \frac{A_p^2 \cot^2 \theta}{B_p^2}} \begin{pmatrix} \frac{A_p}{B_p} \cot \theta \\ 1 \end{pmatrix}, \quad (20)$$

$$v_2 = \sqrt{1 + \frac{A_p^2 \tan^2 \theta}{B_p^2}} \begin{pmatrix} -\frac{A_p}{B_p} \tan \theta \\ 1 \end{pmatrix}, \quad (21)$$

Therefore the mixing angle θ can be extracted from $v_{1,2}$.

The fit results with statistic errors on different ensembles are shown in the second panel of Tabel III. As discussed above, we can also extrapolate the mixing angles and masses from different ensembles to their physical values, illustrated as Fig.5. The comparison of the extrapolated results as well as the PDG averaged ones are also listed in Tabel III. One can see that the extrapolated results highly agree with the ones from the correlated matrix fit. The estimation of systematic uncertainties is similar to the above discussions.

With the extrapolation uncertainties taken into account, we find the mixing angle is:

$$\theta = (1.220 \pm 0.130 \pm 0.010)^\circ, \quad (22)$$

which is consistent with Eq. (17) within the uncertainty. This value is much smaller than the model result extracted from experimental data on weak decays [9–11, 32], and thus insufficient to explain the large SU(3) symmetry breaking effects found in charmed baryon decays. Other mechanisms such as QED corrections should be included.

VI. CHARM QUARK MASS DEPENDENCE

In HQET, the mixing between Ξ_c and Ξ'_c would vanish in the heavy-quark limit. In this limit, the angular momentum J of the light quark pairs becomes a conserved quantum number, hence the flavor eigenstate which the angular momentum of light degrees of freedom has an unambiguous value would coincide with the energy states. In reality, the mixing occurs through a finite quark mass correction and thus is proportional to $1/m_c$ [33, 34].

In this section, we also investigate the charm quark mass dependence of the mixing angle. In practice, we use the ensemble C11P29S to generate the correlation function matrices with several bare charm quark masses around the physical one. By applying the correlated matrix fits for each case, we obtain the results in Table IV. As one can see, the mixing angle decreases with the increase of charm quark mass, which is within our expectation.

In order to investigate the heavy quark mass dependence of the mixing angle, and furthermore to predict the behavior at heavy quark limit, we employ a roughly fit ansatz for the mixing angle θ as a function of m_{Ξ_c}

$$\theta = \frac{B_1}{m_{\Xi_c}} + \frac{B_2}{m_{\Xi_c}^2}. \quad (23)$$

The results obtained from fit are $B_1 = -2.78(52)\text{GeV}$ and $B_2 = 12.9(1.3)\text{GeV}^2$ with $\chi^2/\text{d.o.f} = 0.11$. It should be noticed that the value of $B_{1,2}$ would suffer from sizeable discretization effects due to the ensemble we used for this investigation.

	m_{Ξ_c} (GeV)	$m_{\Xi'_c}$ (GeV)	$\chi^2/\text{d.o.f}$	θ (°)	$\chi^2/\text{d.o.f}$	fit range (fm)
C11P14L	2.4315(37)	2.5289(50)	0.69	1.095(88)	0.81	1.51 – 2.81
C11P22M	2.4386(48)	2.5361(62)	0.76	1.075(76)	0.93	1.30 – 2.81
C11P29S	2.4659(44)	2.5673(57)	0.76	1.094(60)	1.1	1.30 – 2.81
C08P30S	2.4678(30)	2.5852(38)	1.0	1.225(52)	0.89	1.20 – 2.40
C06P30S	2.4658(31)	2.5884(36)	1.4	1.212(55)	1.0	1.26 – 1.92
Extrapolated	2.4230(100) _{stat} (194) _{syst}	2.5430(130) _{stat} (255) _{syst}		1.22(13) _{stat} (1) _{syst}		
Exp. data [29]	2.46794 ^{+0.00017} _{-0.00020}	2.5784 ± 0.0005		—		

TABLE III. Results of masses from GEVP eigenvalues, and of mixing angles from eigenvectors on different ensembles, together with $\chi^2/\text{d.o.f}$ of each independent fits and the fit ranges. The following are extrapolated results, and the PDG-averaged ones are also listed here for comparison.

m_c^b	0.2	0.3	0.4	0.44	0.478	0.5	0.6	0.7	0.8
m_{Ξ_c} (GeV)	2.0987(25)	2.2380(28)	2.3594(26)	2.4069(26)	2.4587(27)	2.4793(29)	2.5878(30)	2.6898(30)	2.7859(31)
$m_{\Xi'_c}$ (GeV)	2.1834(24)	2.3249(29)	2.4514(24)	2.4999(24)	2.5536(29)	2.5718(29)	2.6823(29)	2.7859(30)	2.8835(30)
θ (°)	1.639(75)	1.349(73)	1.116(49)	1.049(46)	1.002(50)	0.969(53)	0.847(47)	0.751(42)	0.674(39)

TABLE IV. Results of m_{Ξ_c} , $m_{\Xi'_c}$ and θ at different bare charm quark masses. The bold ones correspond to a physical charm quark. These results are extracted from the correlated fit of the correlation function matrix on C11P29S. The total measurements of non-physical mass cases are $N_{\text{meas}} = 432 \times 14$. Uncertainties in all results are statistical only.

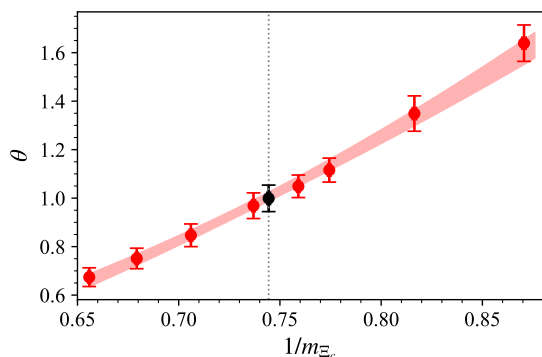


FIG. 6. Mixing angle θ as a function of $1/m_{\Xi_c}$. The red data points denote the results based on unphysical charm quark masses, and the black data point denotes the physical one. Uncertainties in all data points are statistical only.

VII. SUMMARY

In summary, we have explored the Ξ_c - Ξ'_c mixing by calculating the two-point correlation functions of the operators to interpolate the Ξ_c and Ξ'_c baryons from the lattice QCD. Based on the lattice data, we have adopted two independent methods to determine the mixing angle between Ξ_c and Ξ'_c . Direct analysis of the correlation function is conducted and a small mixing angle is found.

This observation is also confirmed through the analysis of solving the generalized eigenvalue problem.

After making the chiral and continuum extrapolation, we found that the mixing angle θ is $1.2^\circ \pm 0.1^\circ$, which is significantly small than the ones from other methods. This indicates the Ξ_c - Ξ'_c mixing is insufficient to account for the large SU(3) symmetry-breaking effects found in weak decays of charmed baryons, and further mechanisms are required. A combined investigation of Λ_c and Ξ_c decay form factors from lattice QCD that include the mixing effects is undergoing.

ACKNOWLEDGEMENT

We are grateful to Fengkun Guo, Xiao-Gang He, Jiajun Wu, and Qiang Zhao for useful discussions. This work is supported in part by Natural Science Foundation of China under grant No. U2032102, 12061131006, 12125503, 12293060, 12293061, 12293062. The LQCD calculations were performed using the Chroma software suite [35] and QUDA [36–38] through HIP programming model [39]. The computations in this paper were run on the Siyuan-1 cluster supported by the Center for High Performance Computing at Shanghai Jiao Tong University, and Advanced Computing East China Sub-center.

[1] N. Isgur and M. B. Wise, Phys. Lett. B **232**, 113-117 (1989) doi:10.1016/0370-2693(89)90566-2

[2] N. Isgur and M. B. Wise, Phys. Rev. Lett. **66**, 1130-1133 (1991) doi:10.1103/PhysRevLett.66.1130

- [3] M. Ablikim *et al.* [BESIII], Phys. Rev. Lett. **115**, no.22, 221805 (2015) doi:10.1103/PhysRevLett.115.221805 [arXiv:1510.02610 [hep-ex]].
- [4] M. Ablikim *et al.* [BESIII], Phys. Lett. B **767**, 42-47 (2017) doi:10.1016/j.physletb.2017.01.047 [arXiv:1611.04382 [hep-ex]].
- [5] S. Meinel, Phys. Rev. Lett. **118**, no.8, 082001 (2017) doi:10.1103/PhysRevLett.118.082001 [arXiv:1611.09696 [hep-lat]].
- [6] Y. B. Li *et al.* [Belle], Phys. Rev. Lett. **127**, no.12, 121803 (2021) doi:10.1103/PhysRevLett.127.121803 [arXiv:2103.06496 [hep-ex]].
- [7] Q. A. Zhang, J. Hua, F. Huang, R. Li, Y. Li, C. Lü, C. D. Lu, P. Sun, W. Sun and W. Wang, *et al.* Chin. Phys. C **46**, no.1, 011002 (2022) doi:10.1088/1674-1137/ac2b12 [arXiv:2103.07064 [hep-lat]].
- [8] X. G. He, F. Huang, W. Wang and Z. P. Xing, Phys. Lett. B **823**, 136765 (2021) doi:10.1016/j.physletb.2021.136765 [arXiv:2110.04179 [hep-ph]].
- [9] C. Q. Geng, X. N. Jin and C. W. Liu, Phys. Lett. B **838**, 137736 (2023) doi:10.1016/j.physletb.2023.137736 [arXiv:2210.07211 [hep-ph]].
- [10] C. Q. Geng, X. N. Jin, C. W. Liu, X. Yu and A. W. Zhou, Phys. Lett. B **839**, 137831 (2023) doi:10.1016/j.physletb.2023.137831 [arXiv:2212.02971 [hep-ph]].
- [11] H. W. Ke and X. Q. Li, Phys. Rev. D **105**, no.9, 9 (2022) doi:10.1103/PhysRevD.105.096011 [arXiv:2203.10352 [hep-ph]].
- [12] T. M. Aliev, A. Ozpineci and V. Zamiralov, Phys. Rev. D **83**, 016008 (2011) doi:10.1103/PhysRevD.83.016008 [arXiv:1007.0814 [hep-ph]].
- [13] Y. Matsui, Nucl. Phys. A **1008**, 122139 (2021) doi:10.1016/j.nuclphysa.2021.122139 [arXiv:2011.09653 [hep-ph]].
- [14] Z. S. Brown, W. Detmold, S. Meinel and K. Orginos, Phys. Rev. D **90**, no.9, 094507 (2014) doi:10.1103/PhysRevD.90.094507 [arXiv:1409.0497 [hep-lat]].
- [15] J. Franklin, Phys. Rev. D **55**, 425-426 (1997) doi:10.1103/PhysRevD.55.425 [arXiv:hep-ph/9606326 [hep-ph]].
- [16] H. Bahtiyar, K. U. Can, G. Erkol, M. Oka and T. T. Takahashi, Phys. Lett. B **772**, 121-126 (2017) doi:10.1016/j.physletb.2017.06.022 [arXiv:1612.05722 [hep-lat]].
- [17] K. Ott nad *et al.* [ETM], JHEP **11**, 048 (2012) doi:10.1007/JHEP11(2012)048 [arXiv:1206.6719 [hep-lat]].
- [18] C. Michael *et al.* [ETM], Phys. Rev. Lett. **111**, no.18, 181602 (2013) doi:10.1103/PhysRevLett.111.181602 [arXiv:1310.1207 [hep-lat]].
- [19] J. F. Simeth,
- [20] Z. R. Kordova,
- [21] Z. R. Kordova *et al.* [CSSM/QCDSF/UKQCD], Phys. Rev. D **104**, no.11, 114514 (2021) doi:10.1103/PhysRevD.104.114514 [arXiv:2110.11533 [hep-lat]].
- [22] G. S. Bali *et al.* [RQCD], JHEP **08**, 137 (2021) doi:10.1007/JHEP08(2021)137 [arXiv:2106.05398 [hep-lat]].
- [23] K. Ott nad *et al.* [ETM], Phys. Rev. D **97**, no.5, 054508 (2018) doi:10.1103/PhysRevD.97.054508 [arXiv:1710.07986 [hep-lat]].
- [24] K. Ott nad *et al.* [OTM], Nucl. Phys. B **896**, 470-492 (2015) doi:10.1016/j.nuclphysb.2015.05.001 [arXiv:1501.02645 [hep-lat]].
- [25] A. G. Grozin and O. I. Yakovlev, Phys. Lett. B **285**, 254-262 (1992) doi:10.1016/0370-2693(92)91462-I [arXiv:hep-ph/9908364 [hep-ph]].
- [26] G. Wang *et al.* [χ QCD], Phys. Rev. D **106**, no.1, 014512 (2022) doi:10.1103/PhysRevD.106.014512 [arXiv:2111.09329 [hep-lat]].
- [27] H. Liu, J. He, L. Liu, P. Sun, W. Wang, Y. B. Yang and Q. A. Zhang, [arXiv:2207.00183 [hep-lat]].
- [28] H. Xing, J. Liang, L. Liu, P. Sun and Y. B. Yang, [arXiv:2210.08555 [hep-lat]].
- [29] R. L. Workman *et al.* [Particle Data Group], PTEP **2022**, 083C01 (2022) doi:10.1093/ptep/ptac097
- [30] J. J. Dudek, R. G. Edwards, M. J. Pardon, D. G. Richards and C. E. Thomas, Phys. Rev. D **82**, 034508 (2010) doi:10.1103/PhysRevD.82.034508 [arXiv:1004.4930 [hep-ph]].
- [31] B. Blossier, M. Della Morte, G. von Hippel, T. Mendes and R. Sommer, JHEP **04**, 094 (2009) doi:10.1088/1126-6708/2009/04/094 [arXiv:0902.1265 [hep-lat]].
- [32] Z. P. Xing and Y. j. Shi, [arXiv:2212.09003 [hep-ph]].
- [33] A. F. Falk and M. Neubert, Phys. Rev. D **47**, 2965-2981 (1993) doi:10.1103/PhysRevD.47.2965 [arXiv:hep-ph/9209268 [hep-ph]].
- [34] A. F. Falk and M. Neubert, Phys. Rev. D **47**, 2982-2990 (1993) doi:10.1103/PhysRevD.47.2982 [arXiv:hep-ph/9209269 [hep-ph]].
- [35] R. G. Edwards *et al.* [SciDAC, LHPC and UKQCD], Nucl. Phys. B Proc. Suppl. **140**, 832 (2005) doi:10.1016/j.nuclphysbps.2004.11.254 [arXiv:hep-lat/0409003 [hep-lat]].
- [36] M. A. Clark, R. Babich, K. Barros, R. C. Brower and C. Rebbi, Comput. Phys. Commun. **181**, 1517-1528 (2010) doi:10.1016/j.cpc.2010.05.002 [arXiv:0911.3191 [hep-lat]].
- [37] R. Babich, M. A. Clark, B. Joo, G. Shi, R. C. Brower and S. Gottlieb, doi:10.1145/2063384.2063478 [arXiv:1109.2935 [hep-lat]].
- [38] M. A. Clark, B. Joó, A. Strelchenko, M. Cheng, A. Gambhir and R. Brower, [arXiv:1612.07873 [hep-lat]].
- [39] Y. J. Bi, Y. Xiao, W. Y. Guo, M. Gong, P. Sun, S. Xu and Y. B. Yang, PoS **LATTICE2019**, 286 (2020) doi:10.22323/1.363.0286 [arXiv:2001.05706 [hep-lat]].